



Seismic velocity images of a crystallized crustal magma-conduit (related to the Deccan plume) below the seismically active Kachchh rift zone, Gujarat, India

Prantik Mandal¹

Received: 12 April 2021 / Accepted: 16 September 2021 / Published online: 28 September 2021
© The Author(s), under exclusive licence to Springer Nature B.V. 2021

Abstract

Local earthquake seismic tomography of the Kachchh rift zone (India) using arrival times of P- and S-waves detect a semi-circular region of lower seismic velocities (8–15% drop in V_p and 10–20% drop in V_s) down to 10 km depth and increased seismic velocities (10–17% increase in V_p as well as V_s) between 10 and 40 km depths, which spatially correlates well with the areas of earliest alkaline magmatism related to the Deccan plume, in the SW part of the Kachchh rift. The occurrence of ultramafic xenoliths and tholeiitic basalts in the region suggests a direct link of this magmatism with the initial stage of Deccan plume. Thus, the mapped anomaly might be indicating the presence of imprints of a crystallized magma-conduit related to the 65 Ma Deccan mantle plume. This plume model gets further support from the modelled crustal and asthenospheric thinning below this anomaly, from earlier studies. Relocations of majority of $M \geq 5$ events (including the 2001 mainshock and the 1956 Anjar event) fall within this semi-circular crustal anomaly. Most of these $M \geq 5$ events are observed to occur near the contacts between high- and low-velocity zones while some earthquakes (including the 1956 Anjar earthquake) also occurred in the low-velocity zones (8–18% drop in V_p and V_s , indicating the presence of aqueous/metamorphic fluids). We propose that mapping of such a scenario of crustal and lithospheric structure where resultant tectonic forces encourage seismicity is crucial for the assessment of the intraplate seismic hazard.

Keywords Tomography · Vertical Tectonics · Horizontal Tectonics · Mafic plutons · Joint inversion · Converted phases

1 Introduction

Mid-plate earthquakes do generally concentrate in pre-existing weak fault zones with large return periods, away from active tectonic plate boundaries (Bruckner 1989; Weingarten et al. 2015; Mandal et al. 1997). Numerous studies have already established the fact that

✉ Prantik Mandal
prantikmandal62@gmail.com

¹ Seismological Imaging Group, CSIR-National Geophysical Research Institute, Uppal Road, Hyderabad Telangana-500007, India

the horizontal regional plate tectonic forces are not the dominant causative forces, which result in sudden stress perturbation along the ancient faults to generate mid-plate earthquakes, away from the active plate boundaries (Mandal et al. 1997; Johnston and Kanter 1990; Zoback and Richardson 1996; Zoback 1992). The spatial distribution of in-situ stress tensors for different regions in the world revealed a large lateral variation and localization of stress tensors in discrete zones that cannot be explained by the horizontal regional plate tectonic forces, which alone can give rise to only homogeneous uniform stress-state over a large region that fails to explain the occurrences of intraplate earthquakes along only some ancient faults but not all of them (Zoback and Richardson 1996; Zoback 1992). This observation supports the idea that localization of stresses due to thickening and thinning of crust, metamorphism, magmatism, and such other multiple tectonic events over the geologic history control the future locations of seismic failures in the intraplate regions (Mandal et al. 1997; Johnston and Kanter 1990; Zoback and Richardson 1996).

Most of the major Indian intraplate earthquakes (viz. 1819 Kachchh, 2001 Bhuj, 1993 Latur, 1967 Koyna) are found to occur in regions, which were influenced by the Deccan volcanism of 65 Ma. The Deccan basaltic outpouring took place when the Indian plate moved over the Re-union hotspot (Courtilot et al. 1986). The Deccan event was associated with a mantle plume that has altered significantly the petrology and geochemistry associated with crust and lithosphere below the Deccan volcanic province covering a huge 0.5 million sq.km. area of the Indian sub-continent (Courtilot et al. 1986; Kennett and Widiyantoro 1999). Thus, the study of the influence of Deccan volcanism event on the crust and upper mantle structure below the seismically active intraplate regions can provide important clues to understand the seismogenesis of the Indian intraplate earthquakes occurring in Kachchh, Gujarat, in particular and Indian sub-continent, in general.

The influence of Deccan plume on crustal and lithospheric structures in seismically active Indian intraplate earthquake regions (viz., the 2001 M_w 7.7 Bhuj, 1997 M_w 5.9 Jabalpur, 1993 M_w 6.3 Latur, and 1967 M_w 6.2 Koyna) has been mapped as evidenced by the presence of high velocity lower- and sub-crustal magmatic/under-plated layers, through active and passive imaging studies (Rajendran and Rajendran 1998; Kaila and Sain 1997; Mandal and Pandey 2011; Mandal 2019), which might have been playing a key role in accumulating large intraplate stresses below these regions (Fig. 1; Mandal et al. 1997; Johnston and Kanter 1990; Zoback and Richardson 1996; Zoback 1992; Rajendran and Rajendran 1998; Mandal and Pandey 2011; Mandal 2019, 1999). In 1993, a typical intraplate event of M_w 6.3 occurred at Latur (Maharashtra) along a NW–SE trending south-dipping reverse fault at 7 km depth (Mandal et al. 1997; Gupta et al. 1996, 1998 and 1999). This earthquake claimed a death toll of 10,000 people (Gupta et al. 1996). Several cases of reservoir-induced seismicity with the occurrences of moderate earthquakes (M 5.0–6.3) have been noticed along the Western Ghats, including the most intriguing site of reservoir triggered seismicity since 1961, at Koyna (Gupta 1992). Besides, several cases of swarm earthquake activity have been noticed in the Deccan volcanic province of Maharashtra and Gujarat (Mahesh and Gupta 2016; Srinagesh et al. 2012). Further, two intraplate rift zones of India (viz. Narmada–Son and Kachchh rift zones) have been evidenced by the occurrences of lower-crustal earthquakes (like the 2001 M_w 7.7 Bhuj and 1997 M_w 5.8 Jabalpur earthquakes), which have been explained by the accumulation of large stresses due to the presence of mafic plutons and rift pillow below these rift zones (Rajendran and Rajendran 1998; Mandal 2019). The occurrence of the 1970 Broach thrust earthquake (Fig. 1) has been associated with the movement along the NSL (Fig. 1) related to the upliftment of the region due to the continued northward movement of the Indian plate (Gupta et al. 1972; Kothiyari and Rastogi 2013). Further, the generation of large intraplate earthquakes in India

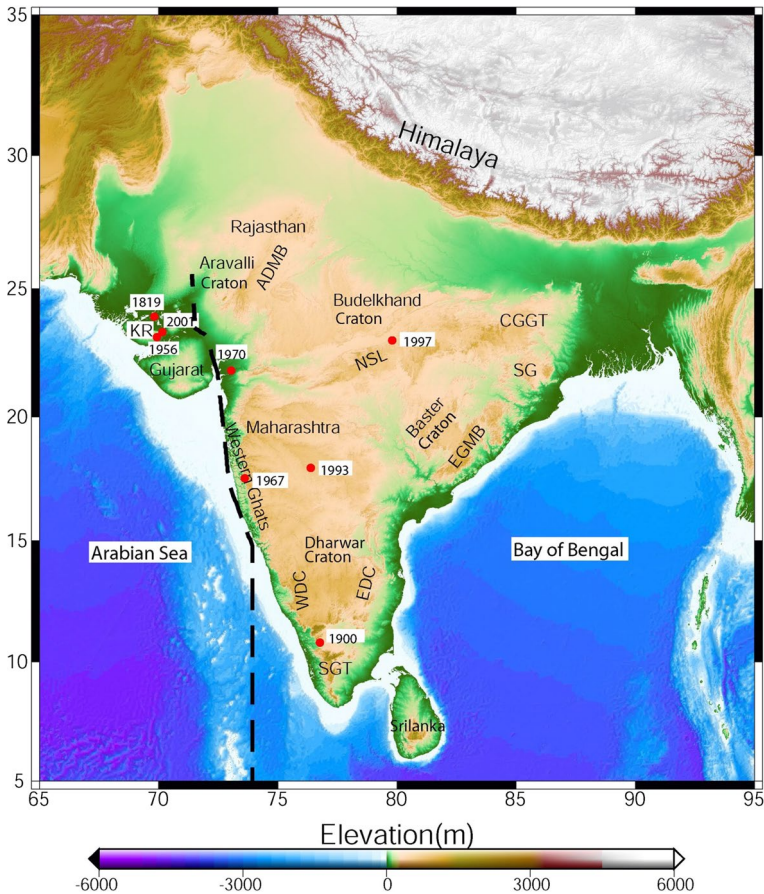


Fig. 1 Elevation (in m) map of India, showing six major Archean cratons viz., Aravalli, Bundelkhand, Singhbhum, Bastar, Dharwar and SGT (southern granulite terrain). The Dharwar craton (DC) comprises of EDC (eastern Dharwar craton), WDC (western Dharwar craton). CGGT marks the Chotanagpur granitic gneissic terrain (CGGT) while ADMB represents Aravalli-Delhi mobile belt. The KR and NSL mark the locations of two rift zones viz., Kachchh rift and Narmada–Son lineament. The locations of Maharashtra, Gujarat, Rajasthan, and western Ghats are also shown. A thick black dashed line marks the Deccan plume track based on the ages of the Deccan flood basalts (Sheth, 2005). Solid filled red circles represent locations of significant intraplate earthquakes in India. Figure 1 is generated using the Generic Mapping Tool (GMT) software version 6 (Wessel et al. 2019; <https://doi.org/10.1029/2019GC008515>). The elevation data used in generating GMT plot is obtained from the open source Digital Elevation Model (DEM) (<https://asterweb.jpl.nasa.gov/gdem.asp>)

has also been explained in terms of lithospheric buckling of the Indian lithosphere due to the northward movement of the Indian plate (Bendick and Bilham 1999; Vita-Finzi 2004). But, observed significant changes in the orientation of in-situ principal stress tensor do not show a uniform stress-state over the whole Indian sub-continent, suggesting the importance of local tectonic forces in controlling the stress-state of the Indian plate (Coblentz et al. 1998; Gowd et al. 1992). The zones of upliftment/subsidence along the Western Ghats have been modelled using data from tide gauges, levelling, geomorphology, and erosion (Bruckner 1989; Bendick and Bilham 1999; Chamyal et al. 2002). However, the

erosion/upliftment cannot explain the change in orientations of principal stress tensor over the Indian sub-continent (Vita-Finzi 2004). Moreover, 3-D modelling of stresses induced by topography and crustal density heterogeneities suggest sizable deviatoric stresses of 100 MPa, which also might be controlling the spatial locations of earthquake occurrences in different parts of Peninsular India (Mandal et al. 1997; Mandal 1999, 2019). This further supports the idea that vertical tectonics is playing a key role in the localization of stress-state over the Indian sub-continent, thus, the horizontal regional plate tectonic forces are not the only controlling factor (Fig. 2).

The horizontal and vertical tectonic forces can only induce large stresses in relatively more heterogeneous crustal intraplate regions, which are away from plate boundaries, but they cannot provide the required triggering to nucleate earthquakes. In continents, deep structures also play a key role in generating large intraplate earthquakes. Tomography and other geophysical studies in several large Indian intraplate earthquake regions (e.g. the 2001 Bhuj, 1993 Latur, and 1967 Koyna) have confirmed the role of fluids in earthquake generation (Gupta et al. 1998, 1972; Mandal 2019). In Japan, Zhao et al. (1996) have also shown through high-resolution tomography that aqueous fluids in the lower crust have played a key role in triggering the 1995 Kobe earthquake. In New Madrid, USA, the generation of large crustal earthquakes has been found to be largely contributed by stresses associated with the large upper mantle structures (Chen et al. 2014). The seismic hazard in

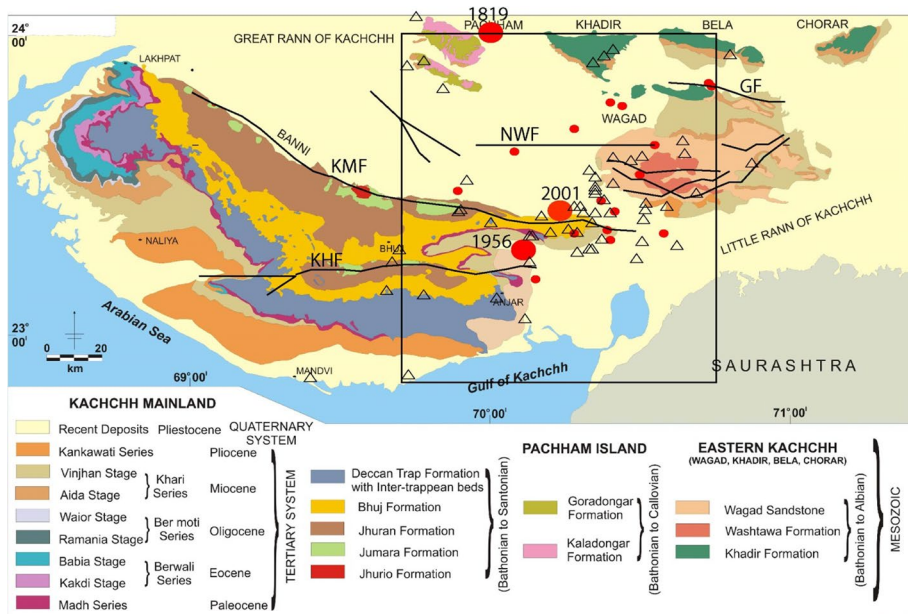


Fig. 2 A map showing distributions of different geological formations in the Kachchh (Gujarat) region. Open black triangles mark the location of broadband stations while small red circles mark the earthquake relocations obtained from simultaneous inversion. The solid black line represents faults. ABF: Allah bund fault; IBF: Island belt fault; NWF: north Wagad fault; GF: Gedi fault; KMF: Kachchh Mainland fault; KHF: Katrol hill fault. Medium filled red circles mark the epicentral locations of $M \geq 5$ events while large filled red circles represent $M \geq 6$ events viz. 1819 Kachchh, 2001 Bhuj, and 1956 Anjar earthquakes (After Biswas 2005). A square area marked by black solid line marks our study area for tomographic experiment (22.9–24°N, 69.7–70.7°E)

intraplate settings has been proposed to be controlled by mantle flows also (Becker et al. 2015).

Here we test the hypothesis that vertical tectonic forces are the main controlling forces to promote failures along the ancient faults in the Kachchh rift zone, Gujarat, India. To achieve the objective, we perform a detailed local earthquake velocity tomography (Benz et al. 1996) of the region, using 24,019 P- and 23,825 S-arrival times of 3750 local earthquakes from 41 stations (Figs. 3a–b, 5a–e). We also construct a 3-D structural model of the rift zone based on estimated thicknesses of sediments, crust, and lithosphere through modelling of Sp and Ps converted phases, from our earlier studies (Figs. 4a–c; “additional figures are given in Online Resource 1”). The results of Vp, Vs, and Vp/Vs tomograms (Figs. 8a–m; “additional figures are given in Online Resource 4”) are used to understand the role of local (vertical) tectonic forces in controlling the uninterrupted generation of earthquakes in the Kachchh rift zone since the occurrence of the 2001 Bhuj mainshock (Figs. 5, 6, 7).

2 Seismotectonics and seismicity of the Kachchh rift zone, Gujarat, India

The Kachchh region of Gujarat, India, hosts three prominent zones of recurrent strain localization and modern seismicity viz. the 1819 M_w 7.8 Allah Bund earthquake, the 1956 M_w 6.0 Anjar earthquake, and the 2001 M_w 7.7 Bhuj earthquake regions (Figs. 1, 2 and 3a; Rajendran et al. 2008). Till date, the region has experienced seven $M \geq 6$ events (Rajendran et al. 2008). Most of these earthquakes have been reported to be associated with the south-dipping reverse faulting, suggesting the region is under compression. Some earthquakes associated with strike-slip faulting have also been reported from the region viz. 7 March 2006 Gedi event of M_w 5.5 with a focal depth of 3 km (“additional table is given in Online Resource 9”). Several half-grabens and E-W trending tectonic faults characterize the region. These favourably oriented faults can accumulate sizable crustal intraplate stresses in response to the prevailing NS compression resulted from the northward motion of the Indian plate (Mandal 2019). A half-graben structure lies below the central portion of the Kachchh rift zone, which is known as the Samkhiyali graben (SG) (Rastogi et al. 2014). Gravity high (+20 mgal) is observed to be associated with the SG while the surrounding horst structure is noticed to be characterized by gravity low (−20 mgal) (Khan et al. 2016). The hard Mesozoic/Jurassic sediments characterize the most of Wagad uplift and Kachchh mainland while Banni in the north and coastal regions in the south are characterized by mostly alluvium/Tertiary formations (Rastogi et al. 2014). Besides, Deccan basalts are found in the southern part of the Kachchh mainland. Topographically, the Kachchh region is made up of east–west trending hill ranges i.e. the island belt, the Kachchh Mainland and the Wagad. But, the E-W trending Kaladongar hill range in the Patchnam uplift (located 80 km north of the Bhuj city) is the highest (~468 m) hill range in the Kachchh. Fault bounded domes and/or faulted anticlines define uplifted blocks in Kachchh. Igneous intrusions, such as laccoliths, plugs, sills and dyke swarms are localized in the faulted margins of the uplifted blocks of Kachchh (Biswas and Deshpande 1973; Biswas 2005, 2016; Rastogi et al. 2014). The tilted blocks form a system of step faults, giving rise to a series of one-sided horsts and half-grabens within the Kachchh basin (Biswas and Deshpande 1973; Biswas 2005). These faults reactivated at certain intervals causing major earthquakes in 1819, 1956 and 2001 (Fig. 1). Presently the strike-slip KMF is overstepped by the SWF

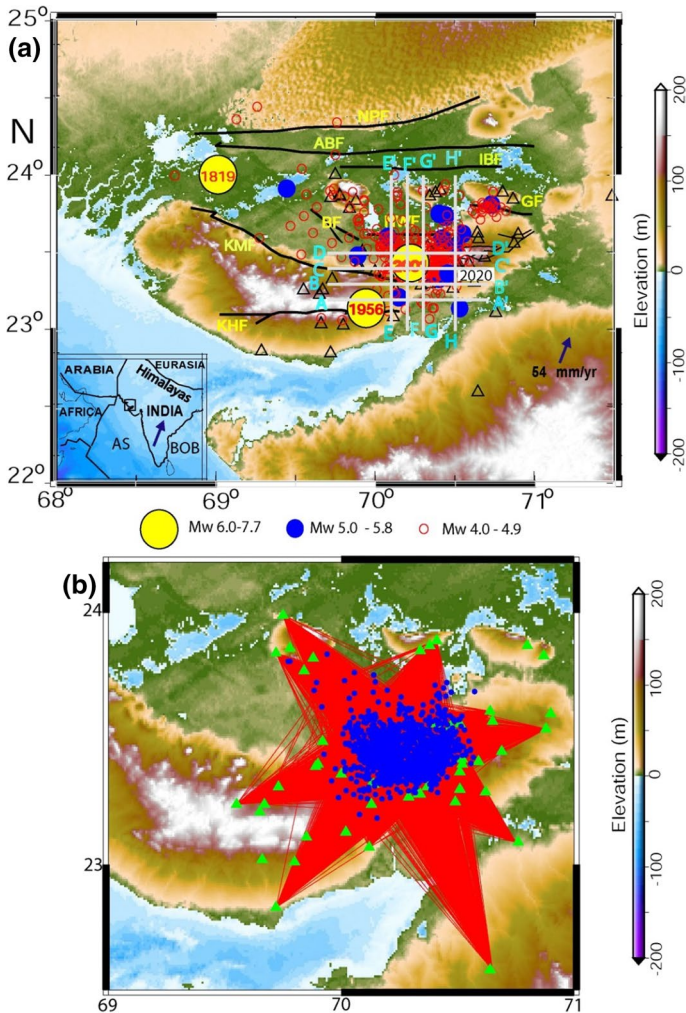


Fig. 3 Station location map of the Kachchh (Gujarat) region. Open black triangles mark the location of broadband stations while small red circles mark the earthquake relocations obtained from simultaneous inversion. The solid black line represents faults. ABF: Allah bund fault; IBF: Island belt fault; NWF: north Wagad fault; GF: Gedi fault; KMF: Kachchh Mainland fault; KHF: Katrol hill fault. Large blue filled circles mark the epicentral locations of $M \geq 5$ events while large filled yellow circles represent $M \geq 6$ events viz. 1819 Kachchh, 2001 Bhuj, and 1956 Anjar earthquakes, and (b) A plot showing ray sampling of the study area for local earthquake velocity tomography. Blue dots mark epicenters while green triangles represent broadband seismograph stations. Figure 2a,b are generated using the Generic Mapping Tool (GMT) software version 6 (Wessel et al. 2019; <https://doi.org/10.1029/2019GC008515>). The elevation data used in generating GMT plot is obtained from the open source Digital Elevation Model (DEM) (<https://asterweb.jpl.nasa.gov/gdem.asp>)

that resulted in the formation of convergent transfer zone undergoing transpressional stress in the strained eastern part of the basin, where large aftershocks and the mainshock of the 2001 Bhuj earthquake sequence took place (Biswas 2005 and 2016; Kothiyari and Rastogi 2013; Kothiyari et al. 2016; Lakhote et al 2021; Rastogi et al. 2014). The tomographic

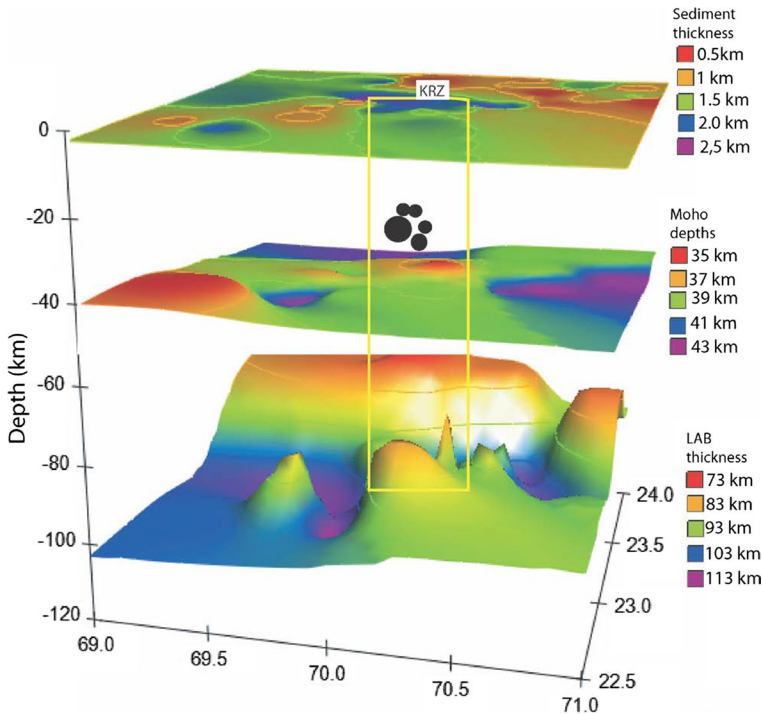


Fig. 4 3-D structural model of the Kachchh rift zone showing surface plots of sediment thickness (in km) (modelled using S-to-p conversions at 53 three-component stations), Moho depths (in km) and lithospheric thicknesses (in km) (modelled through joint inversion of PRFs and surface wave dispersion data). Medium filled black circles mark the $M \geq 5$ events while the 2001 Bhuj mainshock is shown by a large filled black circle. Figure 3 is generated using the demo version of NCSS 2020 statistical software (<https://www.ncss.com>)

studies delineated a mafic pluton at 5–35 km depths below this zone (i.e. Wagad uplift) (Mandal and Pujol 2006; Mandal 2019). The Wagad uplift region is intruded by several dolerite dykes, the prominent amongst them being the Badargadh dyke, the Tranau-Lilpur dyke, and the Khirai dyke (Rastogi et al. 2014). The E-W trending Badargadh dyke is 45 km long, which is the longest dyke in Kachchh. The presence of mafic intrusive, dykes, plugs, horst, graben, and rift tectonics suggest a significant contribution from the vertical tectonic forces in the evolution of these geological features in Kachchh (Biswas and Deshpande 1973; Biswas 2005; Rastogi et al. 2014). The marked thinning of crust and asthenosphere below the central rift zone, which have been modelled by passive seismic imaging studies (Mandal and Pandey 2011; Mandal 2019), further provides the support for the important role played by vertical tectonics in the Geological evolution of the rift zone.

From the above-discussed section and Geology of the region (Fig. 2), it is quite clear that the Kachchh rift zone was affected by the Deccan volcanism, as evidenced by the exposed 65 Ma Deccan basalts in the region west of Anjar extending up to Lakhpat (Biswas and Deshpande 1973; Kothiyari and Rastogi 2013; Rastogi et al. 2014; Biswas 2005; 2016). This model gets further support from the presence of the ultramafic cumulate xenoliths entrained from alkaline lavas in Kachchh (Karmalkar et al. 2008). The Kachchh region was affected by two-phase rifting phases (at 180 and 90 Ma) associated with magmatism

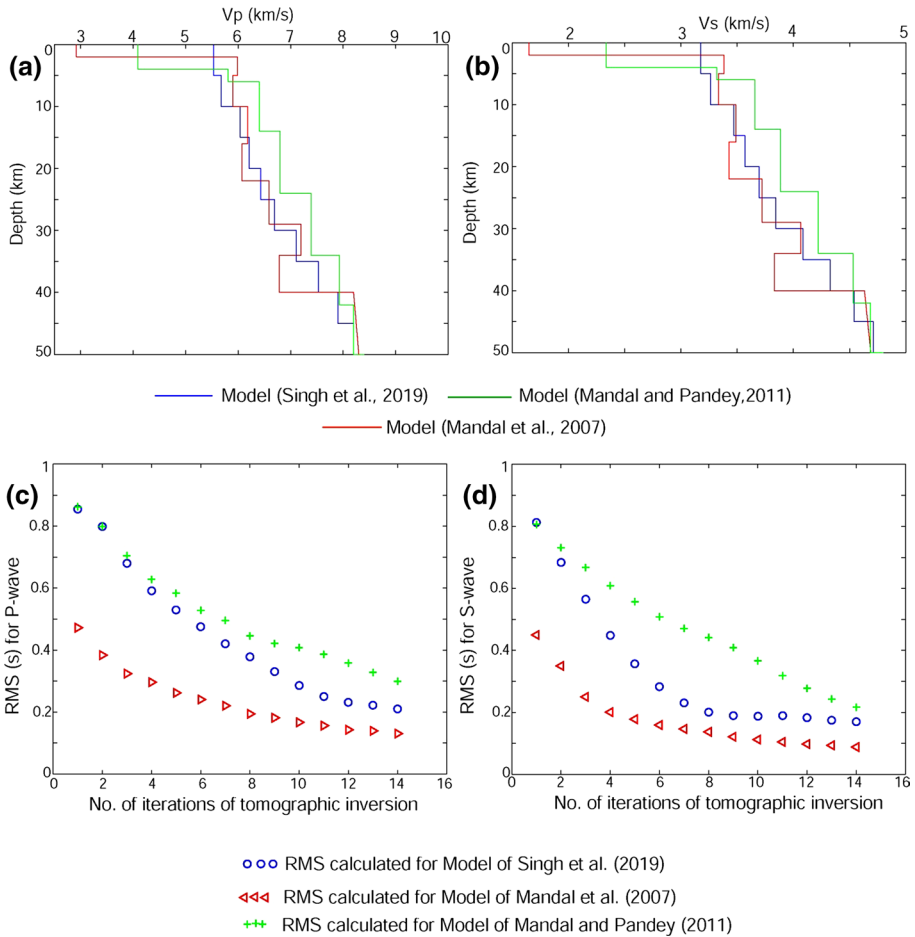


Fig. 5 Three different initial 1-D velocity models used for the tomographic inversion **a** V_p models, **b** V_s models. The variation in RMS values vs. different iterations of the tomographic inversion using above-discussed three different initial models for **c** P-waves and **d** S-waves

episodes. The Kachchh rift basin was formed in Jurassic after the first rifting phase and later the Kachchh rift along with the Indian plate got drifted toward the north during the second rifting phase. Later, the Kachchh rift was influenced by the outpouring of Deccan basaltic lavas at 65 Ma when the Indian plate moved over the Re-Union hotspot (Sheth 2005). The inferred track of the Deccan plume (Sheth 2005) has been shown by a black thick dotted line in Fig. 1. The Geological map (Fig. 2) of the area shows exposed Deccan basalts of 65 Ma in the region between Lakhpat on the northwest to Anjar in the east (Biswas and Deshpande 1973). Seven Deccan lava flows have been identified in Kachchh (De 1981), which are considered to be earliest Deccan eruptions (Medlicott and Blanford 1879; Auden 1949). However, the Deccan trap lava flows are not exposed in the central and northern parts of Kachchh (Kothiyari and Rastogi 2013; Rastogi et al. 2014; Biswas 2005, 2016). But, numerous sills, dykes, plugs have been found in the region north and northwest of the Deccan province in Kachchh, considered to be volcanic centres (Biswas

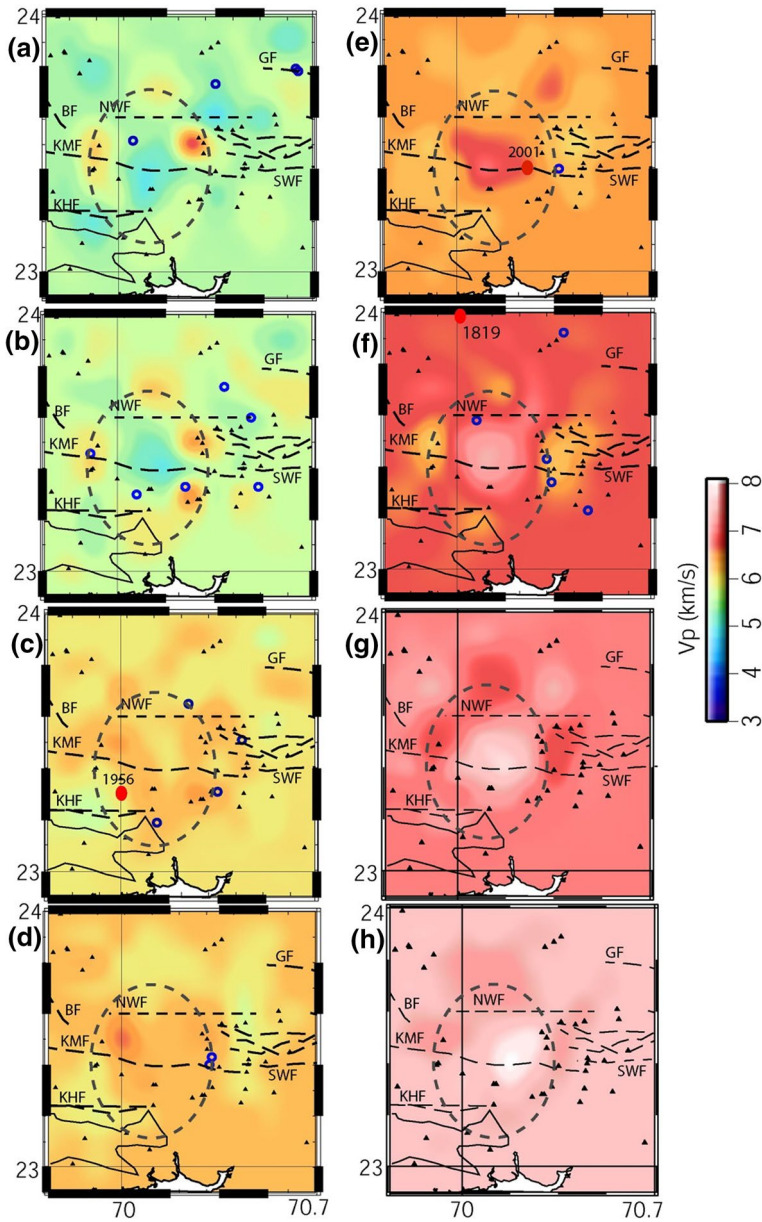


Fig. 6 Horizontal slices of V_p tomograms using the input velocity model of Singh et al. (2019) at **a** 0–5 km, **b** 5–10 km, **c** 10–15 km, **d** 15–20 km, **e** 20–25 km, **f** 25–30 km, **g** 30–35 km, and **h** 35–40 km depth ranges. Thick blue open circles represent the epicentral locations of $M \geq 5$ earthquakes. The large size solid red circles mark the epicentral location of 1819 Kachchh, 1956 Anjar and 2001 Bhuj earthquakes. Thick dotted black lines mark the tectonic faults in the region e.g. north Wagad fault (NWF), south Wagad fault (SWF), Gedi fault (GF), Kachchh mainland fault (KMF), Katrol hill fault (KHF), and Banni fault (BF). Elliptical black dotted lines mark the inferred region affected by the 65 Ma Deccan mantle plume. The zone with exposed Deccan basalts is marked by black solid line. Figures 6a-h are generated using the Generic Mapping Tool (GMT) software version 6 (Wessel et al. 2019)

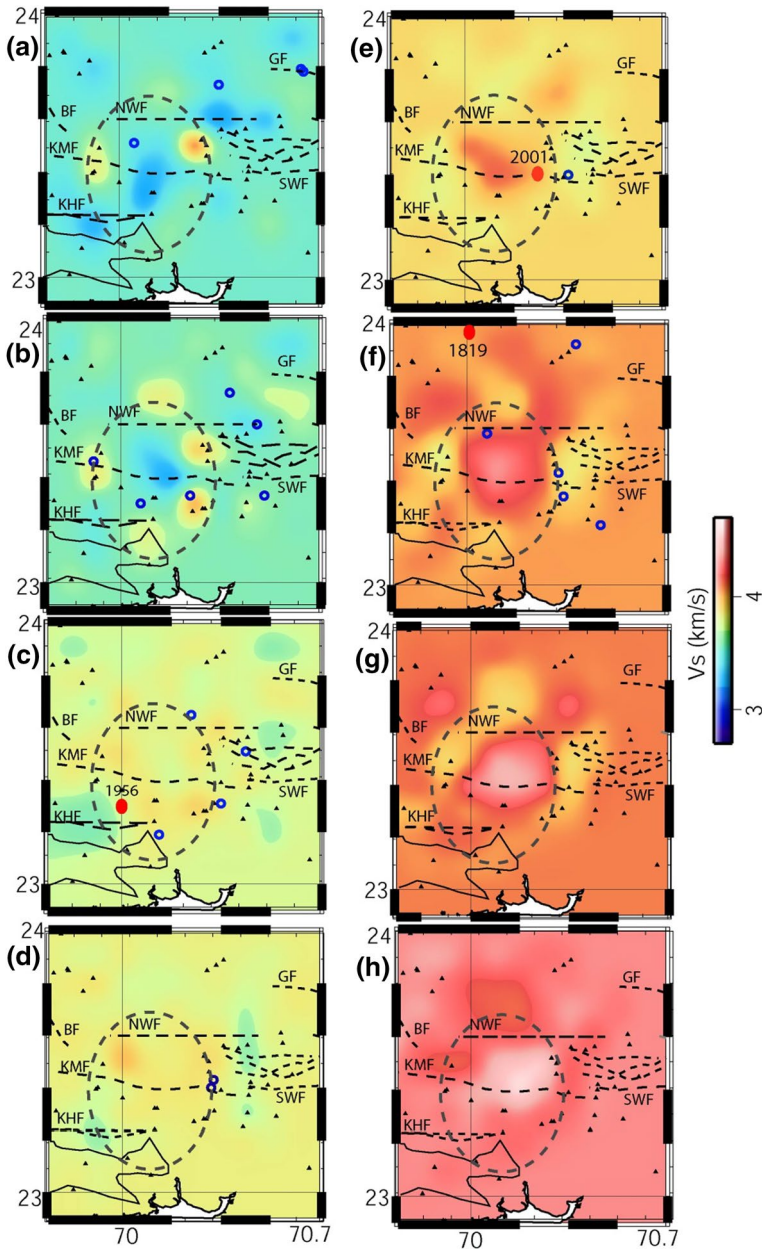


Fig. 7 Horizontal slices of V_s tomograms using the input velocity model of Singh et al. (2019) at **a** 0–5 km, **b** 5–10 km, **c** 10–15 km, **d** 15–20 km, **e** 20–25 km, **f** 25–30 km, **g** 30–35 km, and **h** 35–40 km depth ranges. Thick blue open circles represent the epicentral locations of $M \geq 5$ earthquakes. The large size solid red circles mark the epicentral location of 1819 Kachchh, 1956 Anjar and 2001 Bhuj earthquakes. Thick dotted black lines mark the tectonic faults in the region e.g. north Wagad fault (NWF), south Wagad fault (SWF), Gedi fault (GF), Kachchh mainland fault (KMF), Katrol hill fault (KHF), and Banni fault (BF). Elliptical black dotted lines mark the inferred region affected by the 65 Ma Deccan mantle plume. The zone with exposed Deccan basalts is marked by black solid line. Figures 6a–h are generated using the Generic Mapping Tool (GMT) software version 6 (Wessel et al. 2019)

and Deshpande 1973; Bose 1980; Kothiyari and Rastogi 2013; Rastogi et al. 2014; Biswas 2005, 2016).

3 Methods

3.1 Data and methods

Here we use P- and S-arrival times of 3750 local Bhuj aftershocks (M_w 2.0–5.6), which have been recorded by a close broadband seismic network of 41 three-component seismographs during 2001–2016 in Kachchh, Gujarat that has been deployed by our Institute. Thus, we use 24,019 P- and 23,825 S-wave high-quality arrival times picked from the three-component seismograms of 3750 events and the tomographic technique of Benz et al. (1996) for our local earthquake tomography study. The locations of these earthquakes are shown in Fig. 3a while Fig. 3b shows an excellent sampling of the study region by rays suggesting a good coverage for our local earthquake tomography study. Here, we have performed tomographic inversion using three existing 1-D velocity models as shown in Fig. 5a, b (Mandal 2007; Mandal and Pandey 2011; Singh et al. 2019). The RMS reductions obtained for these three tomographic inversions are shown in Fig. 5c, d, suggesting a more stable RMS reduction for the tomographic inversion using the model of Singh et al. (2019). Thus, the 1-D velocity model of Singh et al. (2019) is considered as the initial velocity model for our 3-D tomographic study (Fig. 5a–b). The relocated earthquakes are found to be occurring mostly in the rupture zones of the 2001 Bhuj mainshock and 2006 Gedi earthquakes.

We use the tomographic inversion code developed by Benz et al. (1996) for our study. The modelling volume is discretized into 16,000 grid nodes, with the volume divided into $40 \times 40 \times 10$ nodes. A uniform horizontal and vertical grid spacing of 5 km was considered in tomographic inversion while for the computation of arrival times and ray tracing a uniform horizontal and vertical grid spacing of 1 km is used (“additional table is given in Online Resource 11”). The smoothing parameter decreases from 50 to 3 together with model roughness decreasing and not affecting the absolute velocities, the RMS residuals for P- and S-waves are reduced from 0.855 s to 0.210 s, and 0.812 s to 0.170 s, respectively, within 14 iterations (Fig. 4c,d). The horizontal slices of V_p , V_s , and V_p/V_s tomograms from 0 to 50 km depths at 5 km depth interval are shown in Figs. 6a–h, 7a–h, with depth cross-sections along four E–W (A, B, C, and D) and four N–S (E, F, G, and H) profiles are shown in “Online Resource 4”. Also, we constructed depth cross-sections of V_p , V_s , and V_p/V_s tomograms along one NW–SE, one NE–SW, one E–W, and one N–S profile across the 2001 Bhuj mainshock to image the nature of crustal structure along and across the strike of the Kachchh seismic zone (Fig. 8a–m). We also compare our tomographic results, which are obtained using 1-D initial velocity model of Singh et al. (2019) (Figs. 6, 7) and, Mandal and Pandey (2011) (“additional figures are given in Online Resource 2–5”) and found that major structural features remain same in both cases. Further, to check the robustness of our results, a synthetic test is performed using the final obtained velocity model at 25 km depth, wherein first synthetic travel times are computed using the final velocity model as the initial model and then the tomographic inversion is performed using the synthetic travel times and same grid parameterization as used in the inversion using observed travel times. The results for V_p and V_s tomography at 25 km depth are shown in “Online Resource 6”, suggesting a more than 90% retrieval of velocity anomaly for both

Fig. 8 Depth sections of tomograms (using the input velocity model of Singh et al. (2019)) along four profiles (PP', QQ', RR' and SS') across the 2001 Bhuj mainshock (marked by solid large grey circle) location (23.4°N, 70.23°E). (a) Elevation (in m) map showing locations of above-mentioned four profiles. Black plus symbol marks seismic stations while white lines mark faults. A filled large grey circle marks the location of 2001 mainshock while a filled pink circle marks the location of the 1956 Anjar earthquake. Along PP' [(23.85°N, 69.7°E) (23.1°N, 70.7°E)] profile (b) Vp, (c) Vs and (d) Vp/Vs. Along QQ' [(23.07°N, 69.9°E) (23.87°N, 70.9°E)] profile (e) Vp, (f) Vs and (g) Vp/Vs. Along RR' [(23.4°N, 69.8°E) (23.4°N, 70.9°E)] profile (h) Vp, (i) Vs and (j) Vp/Vs. and, along SS' [(23.1°N, 70.23°E) (24°N, 70.23°E)] profile (k) Vp, (l) Vs and (m) Vp/Vs. Here, BN, KR, WU, KU, and BU represent Banni, Kachchh rift, Wagad Uplift, Khadir Uplift and Bela Uplift, respectively. The solid thick black line "A" marks the south-dipping NWF, "B" marks the north-dipping KMF, "C" represents the south-dipping BF, "D" marks the south-dipping KHF, and "E" marks the south-dipping GF. Black open circles mark the hypocentral locations of $M \geq 5$ events. Figure 7a is generated using the Generic Mapping Tool (GMT) software version 6 (Wessel et al. 2019). The elevation data used in generating GMT plot is obtained from the open source Digital Elevation Model (DEM) (<https://asterweb.jpl.nasa.gov/gdem.asp>). While Fig. 7b-m are generated using MatlabR2014a (<https://www.mathworks.com/help/matlab>)

Vp and Vs tomography. We also performed checkerboard test by assigning alternately high (+5%) and low-velocity (-5%) perturbations for individual grid nodes in 3-D (Figs. 9a–b; "additional figures are given in "Online Resource 7–8"). Our checkerboard test reveals a 90% retrieval of the Vp and Vs tomograms in the main seismogenic region at 5–10, 10–15, 15–20, 25–30, 30–35 and 35–40 km depths (Figs. 8c–f; "additional figures are given in Online Resource 7–8").

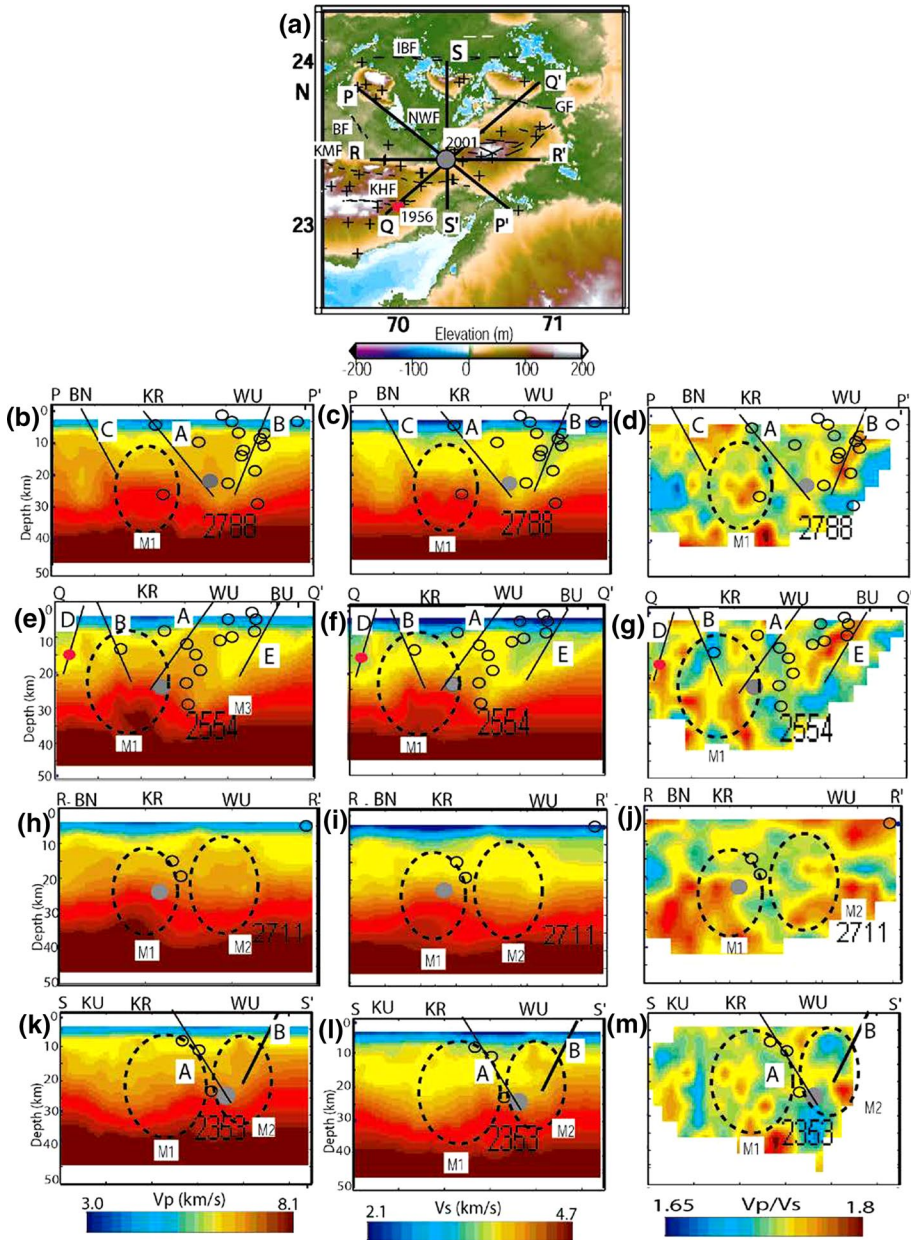
4 Results and discussion

4.1 Thickest sedimentary layer below the central KRZ

The thicknesses of sedimentary layer below the Kachchh rift basin have been modelled at 53 seismic stations by different investigators, using the S-to-p converted phases from the basement/sediment interface (Mandal 2007; Singh et al. 2017). The details of analysis of data to estimate the sediment thickness of the Kachchh basin using Sp converted phase could be found in Mandal (2007) and Singh et al. (2017). The modelled sediment thickness varies from 1.75 to 2.6 km underlying the central Kachchh rift, where most of the $M \geq 4.5$ earthquakes until today including the 2001 $M_w 7.7$ mainshock have occurred (Fig. 3; "additional table is given in Online Resource 9"). While three independent mainshocks of $M \geq 4.5$ took place in the surrounding unrifted zones with sediment thickness of 1.2–1.4 km (Fig. 4; "additional figures are given in Online Resource 1"). Two $M \geq 4.5$ events have also occurred along the Gedi fault, where sediment thicknesses are modelled to be 1.5–1.8 km. Spatial distribution of sediment thicknesses in Fig. 4 also delineates a WNW-ESE rift structure, extending 100 km in length and 40 km in width.

4.2 Marked crustal and lithospheric thinning below the central KRZ

The crustal and lithospheric thicknesses have been modelled at 22 broadband stations in Kachchh, through the joint inversion of PRFs and surface wave group velocity dispersion (5–70 s) data ("additional table is given in Online Resource 10") (Mandal and Pandey 2011; Mandal 2012, 2019). The details of the joint inversion of PRFs and surface wave group velocity dispersion data could be found in Mandal (2012), Mandal (2019), and, Mandal and Pandey (2011). Modelled crustal (lithospheric) thicknesses vary from 37(76)



km below the central rift zone to 43(113) km underlying the surrounding unrifted zones (Fig. 3; “additional table is given in Online Resource 10”). However, the minimum crustal thickness of 35 km is also modelled at MND (near the coastal region) while minimum lithospheric thickness of 76 km is modelled at CHP in the central KRZ (Fig. 4). The crustal thicknesses reveal a significant crustal thinning of 4–6 km below the central rift zone, where three $M \geq 4.5$ earthquakes including the 2001 $M_w 7.7$ mainshock have occurred

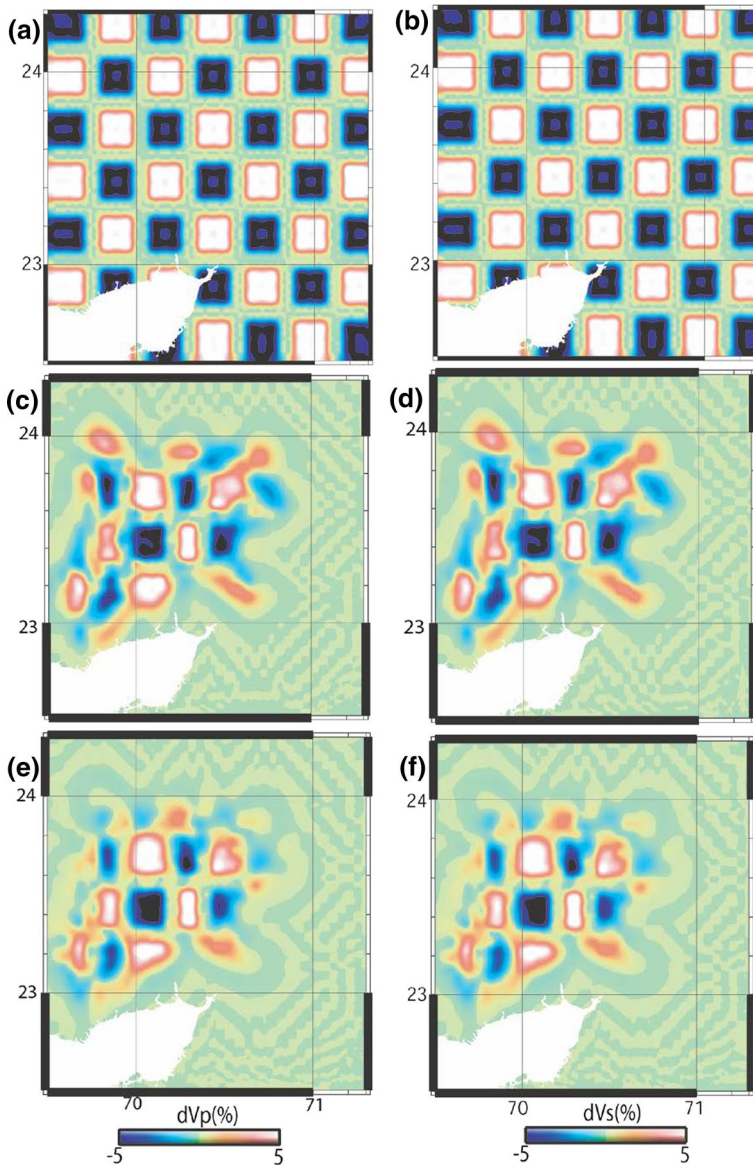


Fig. 9 Results of Checkerboard test. (a,b): Input perturbation model, consisting of 1600 km^3 with velocities 5% compared to the starting model for P- and S- waves, (c,d): recovered perturbation models for P- and S-waves at 5–10 km depths, and (e,f): recovered perturbation models for P- and S- waves at 15–20 km depths. Figure 8a–f are generated using the Generic Mapping Tool (GMT) software version 6 (Wessel et al. 2019)

(Fig. 4; “additional table is given in Online Resource 9”). We also notice that remaining eight earthquakes of $M \geq 4.5$ took place in the surrounding unrifted zones, with a relatively thicker crust. Modelled larger crustal thicknesses (40–43 km) characterize the surrounding unrifted zones (Fig. 3; “additional figures are given in Online Resource 1”). The modelled LAB thicknesses depict a marked asthenospheric upwarping of 6–8 km below the just

southeast corner of the central rift zone (Fig. 4). The modelled marked crustal and asthenospheric thinning provides the evidence for key role played by the vertical tectonic forces in the crustal accretion of the KRZ.

4.3 Three-dimensional lithospheric structural model below the KRZ

We construct a 3-D structural model of the rift zone based on above-discussed estimates of sediment, crustal and lithospheric thicknesses (Fig. 3; “additional figures are given in Online Resource 1”). From this model, it is quite distinctly visible that a lithospheric volume of $50 \times 50 \times 90 \text{ km}^3$ below the central KRZ is significantly influenced by the crustal and asthenospheric thinning, which might be related to the Deccan plume episode of 65 Ma. This lithospheric volume is also observed to be characterized by the thickest sediments ($\sim 2.5 \text{ km}$) of the Kachchh basin (Fig. 4; “additional figures are given in Online Resource 1”). A half-graben structure (i.e. Samkhiyali graben (Biswas 2005; Rastogi et al. 2014)) with a marked gravity high of $+40 \text{ mgal}$ is also found to occur within this lithospheric volume below the central KRZ (Khan et al. 2016). Based on the movements of different existing faults, Biswas (1987) proposed a nucleation zone for the future earthquakes between SWF and Wagad uplift, which also lies within the above-discussed lithospheric volume. Further, we notice that most of the deeper ($> 15 \text{ km}$ depth) earthquakes of $M > 4.5$ in the Kachchh rift zone have occurred within the mapped lithospheric volume (Fig. 4; “additional figures are given in Online Resource 1”). The mapped lithospheric volume seems to be representing a slightly southward dipping crystallized magma-conduit that passes through the zones of marked concentrations of sediment, Moho and LAB contours below the KRZ (Fig. 4). The chemical composition of rocks within this lithospheric column might have been modified significantly, due to the magma interaction during the plume episode. This process might have been increased the densities and velocities of rocks within this lithospheric column by intruding high density and high velocity mafic/ultramafic rocks from the deeper sources. Therefore, this lithospheric column could be acting as a stress accumulator in comparison to the surrounding less affected blocks.

4.4 Local earthquake seismic velocity tomography

Tomogram slices at different depths (viz., 0–5, 5–10, 10–15, 15–20, 20–25, 25–30, 30–35, and 35–40 km depths) reveal a marked lateral variation of seismic velocities below the central KRZ, indicating the presence of large structural heterogeneities at crustal depths (Figs. 6a–h, 7a–h). V_p and V_s tomograms detect a semi-circular-shaped anomaly at 0–40 km depths below the KRZ. This anomaly characterizes by a domination of low velocity (8–15% drop in V_p and 10–20% drop in V_s) in the main aftershock zone (i.e. central KRZ) in comparison to the surrounding unrifted zones down to 10 km depth (Figs. 6a–h, 7a–h). Further, V_p/V_s tomograms depict larger V_p/V_s values (~ 1.7 – 1.8) in the above-mentioned zone suggesting the presence of fluids (probably meteoric water or wet sediments) (“additional figures are given in Online Resource 4”). Also, moderate velocities are mapped below the region between 5 and 10 km depths (Figs. 6a–h, 7a–h), which might be related to the rigid upper-mid crustal rocks. At 10–40 km depths, V_p and V_s tomograms reveal a domination of higher velocity anomalies (10–17% increase in V_p as well as V_s) within the above-discussed circular anomaly, where V_p/V_s tomograms depict lower values (~ 1.6 – 1.75), suggesting the presence of rigid mafic and ultramafic lower-crustal rocks underlying the KRZ (“additional figures are given in Online Resource 4”). This increase in

seismic velocities might be related to the presence of crustal mafic plutons below the KRZ (Mandal 2019). Several low-velocity zones at 10–40 km depths are also mapped which are interpreted as zones filled with aqueous /metamorphic fluids. This distinct semi-circular anomaly below the central KRZ could be related to the 65 Ma Deccan plume activity, This plume model gets further support from the occurrence of ultramafic xenoliths of both mantle and cumulate (igneous) origin in Sayala Devi plug, Kachchh, Gujarat, which might be related to the earliest Deccan tholeiitic basaltic eruptions (Auden 1949; Karmalkar et al. 2008). Thus, it is inferred that this mapped semi-circular anomaly below the study region might be representing the presence of imprints of a crystallized magma-conduit related to the 65 Ma Deccan mantle plume.

The zone marked by thick solid black line in Figs. 6a–h and 7a–h represent the area with exposed Deccan basalts (west of Anjar) in our study region (Fig. 2; Biswas and Deshpande 1973). The elliptical region marked black dotted line shows the inferred semi-circular anomaly that also covers the easternmost part of the zone with the exposed Deccan basalts (Figs. 2, 6 and 7). The inferred semi-circular anomaly is located northwest of the Deccan basalt province of Kachchh, where numerous dykes, sills, and plugs have been mapped geologically, which might represent volcanic centres during the Deccan mantle plume episode (Biswas and Deshpande 1973; Bose 1980). Note that majority of the $M \geq 5$ aftershocks of the 2001 Bhuj mainshock including the 2001 mainshock of $M_w 7.7$ and the 1956 Anjar earthquake of $M_w 6.1$ have occurred within this inferred semi-circular anomaly. Remaining $M \geq 5$ aftershocks have occurred on the neighbouring faults like GF, IBF, and BF, which could be attributed to the migration of coulomb static stress changes due to the continued seismic loading in the main rupture zone of the 2001 Bhuj mainshock (Mandal et al. 2007; Mandal 2009; To et al. 2006). Here the focal depths of 1819 Kutch 1956 Anjar, and 2001 Bhuj are considered to be 30, 15 and 23 km, respectively (To et al. 2003; Chung and Gao 1995; Antolik and Dregar 2003). V_p and V_s tomograms at 30 km depth (Figs. 6e and 7e) suggest that the 1819 event occurred near the contact between high- and low-velocity anomalies while the 1956 Anjar event took place in a zone of low-velocity (Figs. 6c and 7c). But, the 2001 Bhuj event occurred near a contact between high- and low-velocity anomalies at 23–25 km depths (Figs. 6d and 7d). The zones near the contact between high (mafic rigid rocks) and low (rock matrix filled with aqueous fluids) are generally favourable zones for accumulating large intraplate stresses, thereby, generating large lower-crustal earthquakes. While the low-velocity zones can be attributed to the presence of aqueous or metamorphic fluids and entrapped CO_2 volatiles, which can provide the triggering effect for generating large lower-crustal earthquakes. It is apparent that the inferred semi-circular anomaly in the central part of the Kachchh rift zone might represent the imprints of a crystallized magma-conduit related to the 65 Ma Deccan mantle plume, which might have given rise to the E-W trending Kachchh rift zone. The presence of this relatively weak semi-circular crustal volume below the Kachchh rift zone might be qualifying it to be a unique site for accumulating large strains for generating large lower-crustal intraplate earthquakes, in response to the prevailing N-S compression due to the northward movement of the Indian plate.

Depth cross-sections of V_p , V_s , and V_p/V_s tomograms along four E-W (A, B, C, and D as shown in Fig. 3a) and four N-S (E, F, G, and H as shown in Fig. 3a) profiles are shown in “Online Resource 4”. The E-W depth sections (“additional figures are given in Online Resource 4”) clearly delineate three high-velocity anomalies M1, M2, and M3, which are associated with Banni (BN), Kachchh rift (KR), and Wagad uplift (WU), respectively. While the N-S depth sections (Figs. S4m-x) detect three south-dipping faults (e.g. NWF, KHF, GF) and the north-dipping KMF, which are marked as A, D, E, and B, respectively.

The 2001 mainshock is found to occur on the NWF near a contact between high- and low-velocity zones (“additional figures are given in Online Resource 4”). The imaged two high-velocity anomalies (M1 and M2) are interpreted as crustal mafic plutons. Interestingly, the inferred mafic pluton associated with the Kachchh rift (M1) is modelled to be characterized by high V_p (10–20% increase), high V_s (8–17% increase), and low V_p/V_s (~1.65–1.7), which can be interpreted as comprising of mafic and rigid rocks. While the inferred mafic pluton associated with the WU (M2) are found to be associated with high V_p (10–20% increase), high V_s (8–17% increase) and high V_p/V_s (~1.7–1.8), which are interpreted as consisting of crystallized magma showing high V_p/V_s . The presence of a high velocity magmatic lower-crustal layer (V_p : 6.8–7.8 km/s; V_s : 3.9–4.3 km/s; V_p/V_s : 1.7–1.8) at 20–40 km below the region is clearly delineated from all the NS-EW depth cross-sections, which might have been resulted from the densification of the lower crust during the magmatism episodes associated with two phase rifting (viz. 180 Ma African and 90 Ma Madagascar) and the 65 Ma Deccan mantle plume (Courillot et al. 1986).

We notice that most of the $M \geq 5$ earthquakes including the 2001 Bhuj mainshock have occurred near the contacts between high- and low-velocity zones (Figs. 6a–h, 7a–h; “additional figures are given in Online Resource 4”). The contacts between high-velocity (rigid strong rocks) and low-velocity (fluid-filled weak zones) represent zones of high-stress concentrations, thereby, resulting in the generation of moderate to large earthquakes (Mandal and Pandey 2011; Zhao and Negishi 1998). We also notice occurrences of a few $M \geq 5$ events in high-velocity zones (Figs. 6, 7; “additional figures are given in Online Resource 4”), which probably comprise of rigid and brittle rocks and are capable of accumulating large stresses to generate moderate earthquakes (Mandal and Pandey 2011; Zhao and Negishi 1998; Rastogi et al. 2014; Singh et al. 2019). While some $M \geq 5$ earthquakes including the 1956 Anjar earthquake are found to occur in the low-velocity zones (Figs. 6–8; “additional figures are given in Online Resource 4”). A low-velocity zone (V_p : 5.8–6 km/s; V_s : 3.3–3.5; V_p/V_s : 1.73–1.75) has also been detected at the hypocentral zone (~15 km) of the 1956 Anjar earthquake (Figs. 6c, 7c, 8e–g; “additional figures are given in Online Resource 4”). Mid-lower crustal low-velocity zones could be attributed to the presence of metamorphic fluids or volatile CO_2 (Mandal and Pandey 2011; Zhao and Negishi 1998; Rastogi et al. 2014; Singh et al. 2019; Mandal 2012), which might be playing the key role in triggering moderate intraplate earthquakes like the 1956 Anjar.

We also construct depth sections along four profiles across the 2001 Bhuj mainshock location (viz., PP' in NW–SE, QQ' in NE–SW, RR' in EW, and SS' in NS directions) as shown in Fig. 8a–m. Depth sections along PP', QQ' and SS' profiles (Fig. 8a–f, k–m) clearly image the south-dipping north Wagad fault, which was the causative fault for the 2001 Bhuj mainshock. The depth cross-sections of V_p , V_s , and V_p/V_s tomograms along the profiles PP' and RR' detect high-velocity anomalies (10–20% increase in V_p and V_s) at 5–40 km depths associated with the Kachchh rift (KR), and Wagad uplift (WU) (shown by elliptical black dotted lines M1 and M2 in Fig. 8b–d, h–j). Tomograms along profiles QQ' and SS' map two high-velocity anomalies at 5–40 km depths associated with WU and KR (shown by elliptical black dotted lines M1 and M2 in Fig. 8e–g, k–m). Our modelling also detects low-velocity anomalies at 0–30 km depths, which could be attributed to the presence of meteoric water/ wet sediments at 0–10 km depths and aqueous/metamorphic fluids at 5–30 km depths. The epicentral location of the 1956 M_w 6.0 Anjar event is found to lie in the low-velocity zone, suggesting key role played by crustal fluid flows in triggering its occurrence (“additional figures are given in Online Resource 4”). Depth sections (Fig. 8a–m) also detect another three south-dipping faults (like GF, BF, and KHF) and the north-dipping KMF. Depth sections along PP' profile (Fig. 8a–c) clearly shows the association of

hypocentral locations of $M \geq 5$ events with the north-dipping KMF (marked by “B”) and low-velocity zone (low V_p , low V_s , and high V_p/V_s) at 5–20 km depths, suggesting the key role played by the fluids in generating these events. From Fig. 8a–m, we notice that the 2001 mainshock and some $M \geq 5$ events occurred on the NWF near the contact between high- and low-velocity zones. Some $M \geq 5$ are also observed to occur near the contacts between high- and low-velocity zones below WU, KR, and BU (Fig. 8b–d, e–g, k–m). At shallow depth (0–10 km), some $M \geq 5$ are found to occur in the low-velocity zones below WU and BU (Fig. 8b–j). Our results suggest that the faults like NWF, KMF, and GF are critically stressed due to the presence of high-velocity mafic plutons owing to the in-plane plate compression and are getting triggered due to the crustal fluid flows resulting in continued earthquake generation in the region.

4.5 Probable earthquake generation model in the KRZ

Based on the above-discussed modelling results, we infer that the presence of mapped high-velocity crust (including inferred mafic plutons at 5–30 km depths and lower-crustal high-velocity magmatic layer at 20–40 km depths) might be allowing the accumulation of large crustal stresses/strains in the Kachchh rift zone, which could provide required strain energy to generate continued earthquake activity for last two decades. Also, the prevailing N–S compression due to the northward motion of the Indian plate could contribute to the stress regime associated with the KRZ. Further, the mapped lithospheric volume ($\sim 50 \times 50 \times 90 \text{ km}^3$) below the KRZ, which is characterized by a marked crustal and asthenospheric upwarping, could lead to a stress regime very near to failure. Note that Copley et al. (2011) modelled a low frictional coefficient of 0.08 for a stress drop of 35 MPa at 23 km depth on the causative NWF of the 2001 Bhuj mainshock. The modelling of this low frictional coefficient is performed under the assumption that the compressive stresses associated with the India Asia collision are accommodated by the seismogenic crust extending from surface to a depth of 25–30 km below the KRZ (Copley et al. 2011). Given such a low frictional coefficient and crustal condition, the faults within the seismogenic crustal part of the mapped lithospheric volume underlying the KRZ could get triggered to generate earthquakes, by a small perturbation in stress regime due to any kind of local tectonic forces (like crustal fluid flows (Mandal 2012), static stress migration from neighbouring faults (Mandal et al. 2007), volatile CO_2 emanating from the deep mantle (Mandal 2019) or regional plate tectonic forces. Most of the $M \geq 5$ crustal earthquakes including the 2001 Bhuj mainshock are observed to lie within the seismogenic crustal part of the mapped lithospheric volume. Therefore, our modelling suggests that vertical tectonic forces play a dominant role in inducing stress-state that generates earthquakes in KRZ while regional plate tectonic forces could contribute to the earthquake triggering mechanism only.

5 Conclusions

The present study has shown that the continued occurrences of earthquakes have been taking place between 2 and 40 km depths below the KRZ. This seismic zone lies within a lithospheric volume of $50 \times 50 \times 90 \text{ km}^3$, which has suffered significant deformations as evident from the modelled marked crustal and asthenospheric upwarping that might have been related to the Deccan mantle plume and two rifting episodes (at 180 and 90 Ma). Our study also maps a semi-circular seismic velocity anomaly, which suggests a low-velocity

anomaly (8–15% drop in V_p and 10–20% drop in V_s) at 0–10 km depths while it shows a high velocity (10–17% increase in V_p as well as V_s) anomaly at 10–40 km depths. This semi-circular anomaly, in combination with the occurrence of ultramafic xenoliths of both mantle and cumulate (igneous) origin in Sayala Devi plug in Kachchh, Gujarat, might be indicating the presence of imprints of a crystallized magma-conduit related to the 65 Ma Deccan mantle plume. Spatially both of these mapped lithospheric volume and semi-circular anomaly correlate well. Majority of the $M \geq 5$ Bhuj aftershocks (including the 2001 $M_w 7.7$ Bhuj mainshock) and the 1956 $M_w 6.1$ Anjar earthquake took place within the seismogenic crustal part of this mapped semi-circular anomaly / lithospheric volume. This observation suggests that apparently, these foci of the Kachchh seismicity occur where lithospheric structure enhances crustal deviatoric stresses significantly.

Additionally, the presence of modelled mafic plutons and high velocity lower-crustal magmatic layer would also contribute significantly to bring the crustal deviatoric stresses associated with the KRZ near to the failure. Therefore, any faults within the mapped lithospheric volume below the KRZ could generate earthquakes through a small stress perturbation due to any kind of local tectonic forces (e.g. crustal fluid flows, static stress transfer from the neighbouring faults, volatile CO_2 emanating from the deep mantle etc.) or regional plate tectonic forces. Thus, the present study reveals that the vertical tectonic forces play a key role in elevating deviatoric stresses associated with faults within the rift zone, which generate earthquakes uninterruptedly for the past two decades. While regional horizontal plate tectonic forces could only provide the triggering mechanism for earthquake generation at the KRZ.

Our study demonstrates that lithospheric-scale deviatoric stress could also govern the earthquake rate (long-term strain rate) in intraplate settings in the Indian sub-continent. Thus, the time-independent seismic hazard models in the continental interior should be reinterpreted incorporating this important observation. Presently, the seismic zoning map of any region in the world has been developed based on catalogues of instrumentally recorded felt earthquakes and geological reports of past earthquakes. Thus, in the future, the changes in slip rates associated with known or hypothesized source faults due to local variations in deviatoric stress caused by crustal and lithospheric structures should be incorporated in the preparation of seismic zoning map.

Supplementary Information The online version contains supplementary material available at <https://doi.org/10.1007/s11069-021-05051-7>.

Acknowledgements Authors are grateful to the Director, Council of Scientific and Industrial Research—National Geophysical Research Institute (CSIR-NGRI), Hyderabad, India, for his support and permission to publish this work. Figures were plotted using the Generic Mapping Tool (GMT) software (Wessel et al. 2019; <https://doi.org/10.1029/2019GC008515>). All software and support data related to GMT software are freely accessible and available from this site (www.generic-mapping-tools.org). The elevation data used in generating GMT plots are obtained from the open source Digital Elevation Model (DEM) (<https://asterweb.jpl.nasa.gov/gdem.asp>). The phase data for tomography used in the present work can be obtained from the https://www.ngri.org.in/86454/kach_tomo.zip while PRF data used in the present work can be obtained from the https://www.ngri.org.in/86454/PRF_kach.zip.

References

- Antolik M, Dreger DS (2003) Rupture process of the 26 January 2001 $M_w 7.6$ Bhuj, India, earthquake from teleseismic broadband data. *Bull Seism Soc Am* 93:1235–1248
- Auden JB (1949) Dykes in western India. *Trans Natl Inst Sci India* 111:123–157

- Becker TW, Lowry AR, Faccenna C, Schmandt B, Borsa A, Yu C (2015) Western US intermountain seismicity caused by changes in upper mantle flow. *Nature* 524:458–461
- Bendick R, Bilham R (1999) Search for buckling of the southwest Indian coast related to Himalayan collision. In: Macfarlane, A., Sorkhabi, R.B., Quade, J. (Eds.), *Himalaya and Tibet: Mountain Roots to Mountain Tops*. Geological Society of America Special Paper 328:313–321.
- Benz HM, Chouet BA, Dawson PB, Lahr JC, Page RA, Hole JA (1996) Three-dimensional P and S wave velocity structure of redoubt Volcano, Alaska. *J Geophys Res* 101:8111–8128
- Biswas SK (2005) A review of structure and tectonics of Kutch basin, western India, with special reference to earthquakes. *Curr Sci* 88:1592–1600
- Biswas SK, Deshpande SV (1973) A note on the mode of eruption of Deccan trap lavas with special reference to Kutch. *J Geol Soc Ind* 14:134–141
- Biswas SK (2016) Tectonic framework, structure and tectonic evolution of Kutch basin western India. Special Publication Geol Soc India. <https://doi.org/10.17491/cgsi/2016/105417>
- Bose MK (1980) Alkaline magmatism in the Deccan volcanic province. *J Geol Soc Ind* 21:317–329
- Bruckner H (1989) Late Quaternary shorelines in India. In: Scott DB (ed) *Late Quaternary sea-level correlation and its applications*. Kluwer, Dordrecht, pp 169–194
- Chamyal LS, Maurya DM, Bhandari S, Raj R (2002) Late Quaternary geomorphic evolution of the lower Narmada valley, Western India: implications for neotectonic activity along the Narmada—Son fault. *Geomorphology* 46:177–202
- Chen C, Zhao D, Wu S (2014) Crust and upper mantle structure of the New Madrid Seismic Zone: insight into intraplate earthquakes. *Phys Ear Planet Int* 230:1–14
- Chung WY, Gao H (1995) Source parameters of the Anjar earthquake of July 21, 1956, India and its seismo-tectonic implications for the Kutch rift basin. *Tectonophysics* 242:281–292
- Coblentz DD, Zhou S, Hillis RR, Richardson RM, Sandiford M (1998) Topography, boundary forces, and the Indo-Australian intraplate stress field. *J Geophys Res* 103:919–931
- Copley A, Avouac J-P, Hollingsworth J, Leprince S (2011) The 2001 Mw 7. 6 Bhuj earthquake, low fault friction, and the crustal support of plate driving forces in India. *J Geophys Res*. <https://doi.org/10.1029/2010JB008137>
- Courtillot V, Besse J, Vandamme D, Montigny R, Jaeger JJ, Cappetta H (1986) Deccan flood basalts at the Cretaceous/Tertiary boundary? *Ear Planet Sci Lett* 80:361–374
- De A (1981) Late Mesozoic –lower tertiary magma types of Kutch and Saurashtra. *Mem Geol Soc Ind* 3:327–339
- Gowd TN, Srirama Rao SV, Gaur VK (1992) Tectonic stress field in the Indian subcontinent. *J Geophys Res* 97:11879–11888
- Gupta HK (1992) Reservoir-induced earthquakes. Elsevier Scientific Publishing Co., Amsterdam, p 355
- Gupta HK, Mohan I, Narain H (1972) The Broach earthquake of March 23, 1970. *Bull Seismol Soc Am* 62:47–61
- Gupta HK, Sarma SVS, Harinarayana T, Virupakshi G (1996) Fluids below the hypocentral region of Latur Earthquake, India: Geophysical indicators. *Geophys Res Lett* 23:1569–1572
- Gupta HK, Rao RUM, Srinivasan R, Rao GV, Reddy GK, Dwivedy KK, Banerjee DC, Mohanty R, Satyasaradhi YR (1999) Anatomy of surface rupture zones of two stable continental region earthquakes, 1967 Koyna and 1993 Latur, India. *Geophys Res Lett* 26:1985–1988
- Gupta HK, Dwivedy KK, Banerjee DC, Rao RUM, Rao GV, Srinivasan R (1998) Latur earthquake, Maharashtra, India: a case study of a borehole investigation at a SCR earthquake site. Chapman Conference on Stable Continental Region (SCR) Earthquakes Hyderabad: National Geophysical Research Institute; p. 39–40.
- Johnston AC, Kanter LR (1990) Earthquakes in stable continental crust. *Sci Am* 262:54–68
- Kaila KL, Sain K (1997) Variation of crustal velocity structure in India as determined from DSS studies and their implications on regional tectonics. *J Geol Soc India* 49:395–409
- Karmalkar NR, Kale MG, Duraiswami RA, Jonalgadda M (2008) Magma underplating and storage in the crust-building process beneath the Kutch region, NW India. *Curr Sci* 94:1582–1588
- Kennett BLN, Widiyantoro S (1999) A low seismic wave speed anomaly beneath northwestern India: a seismic signature of the Deccan Plume? *Ear Planet Sci Letts* 165:145–155
- Khan PK, Mohanty SP, Sinha S, Singh D (2016) Occurrences of large-magnitude earthquakes in the Kachchh region, Gujarat, western India: tectonic implications. *Tectonophysics* 679:102–116
- Kothiyari GC, Rastogi BK, Morthekai P, Dumka RK, Kandregula RS (2016) Active segmentation assessment of the tectonically active South Wagad Fault in Kachchh, Western Peninsular India, *Geomorphol* 253(2016):491–507
- Kothiyari GC, Rastogi BK (2013) Tectonic control on drainage network evolution in the upper Narmada valley: implication to neotectonics. *Geograph J Hindawi Publishing Corporation*, pp 1–9

- Lakhote A, Thakkar MG, Kandregula RS, Jani C, Kothiyari GC, Chauhan G (2021) Estimation of active surface deformation in the eastern Kachchh region, western India: application of multi-sensor DInSAR technique. *Quatern Int* 575:130–140
- Mahesh P, Gupta S (2016) The role of crystallized magma and crustal fluids in intraplate seismic activity in Talala region (Saurashtra), Western India: an insight from local earthquake tomography. *Tectonophysics* 690:131–141
- Mandal P (1999) Intraplate stress distribution induced by topography and crustal density heterogeneities: Implications for the generation of shallow focus intraplate earthquakes in the south Indian shield. *Tectonophysics* 302:159–172
- Mandal P (2007) Sediment Thicknesses and Q_s vs. Q_p relations in the Kachchh rift basin, Gujarat, India using Sp converted phases. *Pure Appl Geophys* 164:135–160
- Mandal P (2009) Crustal Shear wave splitting in the Epicentral Zone of the 2001 Mw 7.7 Bhuj Earthquake, Gujarat, India. *J Geodyn* 47:246–258
- Mandal P (2012) Passive source seismic imaging of the crust and upper mantle beneath the 2001 Mw7.7 Bhuj earthquake region, Gujarat. *India Bull Seismol Soc Am* 102:252–266
- Mandal P (2019) A possible origin of intraplate earthquakes in the Kachchh rift zone, India, since the 2001 Mw7.7 Bhuj earthquake. *Jou of Asian Earth-Sci* 170:56–72
- Mandal P, Pandey OP (2011) Seismogenesis of the lower crustal intraplate earthquakes occurring in Kachchh, Gujarat, India. *J Asian Earth-Sci* 42:479–491
- Mandal P, Pujol J (2006) Seismic imaging of the aftershock zone of the 2001 Mw7.7 Bhuj earthquake. *India. Geophys Res Lett* 33:L05309
- Mandal P, Manglik A, Singh RN (1997) Intraplate stress distribution induced by topography and crustal density inhomogeneities beneath the Killari, India, region. *J Geophys Res* 102:11719–11729
- Mandal P, Chadha RK, Raju IP, Kumar N, Satyamurty C, Narsaiah R, Maji A (2007) Coulomb static stress variations in the Kachchh, Gujarat, India: Implications for the occurrences of two recent earthquakes (Mw 5.6) in the 2001 Bhuj earthquake region. *Geophys J Int* 168:281–285
- Medlicott HB, Blanford WT (1879) *A Manual of the geology of India*. Geol. Surv. Off, Calcutta, p 347
- Rajendran CP, Rajendran K, Thakkar M, Goyal B (2008) Assessing the previous activity at the source zone of the 2001 Bhuj earthquake based on the near source and distant paleoseismological indicators. *Journal Geophysical Research* 113:B05311–1–B05311–17.
- Rajendran K, Rajendran CP (1998) Characteristics of the 1997 Jabalpur earthquake and their bearing on its mechanism. *Curr Sci* 74:168–174
- Rastogi BK, Mandal P, Biswas S (2014) Seismogenesis of earthquakes occurring in the ancient rift basin of Kachchh, Western India. In the book on “Intraplate Earthquakes” edited by P. Talwani, Cambridge University Press, 126–161. <https://doi.org/10.1017/CBO9781139628921.007>.
- Sheth HC (2005) From deccan to réunion: no trace of a mantle plume. In: Foulger GR, Natland JH, Presnall DC, and Anderson DL (eds) *Plates, plumes, and paradigms*. Geological Society of America Special Paper, vol 388, pp 477–501
- Singh B, Gupta AK, Mandal P (2017) Sediment thickness and Q_s - Q_p relations in the Kachchh rift basin, India, using converted phases. *Bull Seism Soc Am* 107:2532–2539
- Singh AP, Koulakov I, Kumar MR, Kumar S, Kayal JR (2019) Seismic velocity structure and intraplate seismicity beneath the Deccan Volcanic province of western India. *Phys Ear Planet Int* 287:21–36
- Srinagesh D, Srinivas D, Soloman Raju P, Suresh G, Murthy YVVBSN, Saha S, Sarma ANS, Vijay Kumar T (2012) Causative fault of swarm activity in Nanded city, Maharashtra. *Curr Sci* 103:25–26
- To A, Burgmann R, Pollitz F (2006) Postseismic deformation and stress changes following the 1819 Rann of Kachchh, India earthquake: was the 2001 Bhuj earthquake a triggered event? *Geophys Res Lett* 31:L13609
- Vita-Finzi C (2004) Buckle-controlled seismogenic faulting in peninsular India. *Quatern Sci Rev* 23:2405–2412
- Weingarten M, Ge S, Godt JW, Bekins BA, Rubinstein JL (2015) High-rate injection is associated with the increase in US mid-continent seismicity. *Science* 348:1336–1340
- Wessel P, Luis JF, Ujeda L, Scharroo R, Wobbe F, Smith WHF, Tian D (2019) Generic mapping tools version 6. *Geochem Geophys Geosyst* 20:5556–5564. <https://doi.org/10.1029/2019GC008515>
- Zhao D, Negishi H (1998) The 1995 Kobe earthquake: Seismic image of the source zone and its implications for the rupture nucleation. *Geophys Res Lett* 103:9967–9986
- Zhao D, Kanamori H, Negishi H, Wiens D (1996) Tomography of the source area of the 1995 Kobe earthquake: evidence for fluids at the hypocenter? *Science* 274:1891–1894
- Zoback ML (1992) First—and second-order pattern of stress in the lithosphere: the World stress map project. *J Geophys Res* 97:11703–11728

Zoback ML, Richardson RM (1996) Stress Perturbation associated with the Amazonas and other ancient continental rifts. *J Geophys Res* 101:5459–5475

Publisher's Note Springer Nature remains neutral with regard to jurisdictional claims in published maps and institutional affiliations.